

Solubility of Polycyclic Aromatic Hydrocarbons in Supercritical Carbon Dioxide from 313 K to 523 K and Pressures from 100 bar to 450 bar

David J. Miller* and Steven B. Hawthorne

Energy and Environmental Research Center, University of North Dakota, Grand Forks, North Dakota 58202

Anthony A. Clifford and Shuang Zhu

School of Chemistry, University of Leeds, Leeds LS2 9JT, U.K.

The solubility of pyrene, chrysene, perylene, and benzo[ghi]perylene were determined at temperatures ranging from 313 K to 523 K and pressures from 100 bar to 450 bar in supercritical CO₂. Temperature had a much greater effect on solubility than pressure. For example, increasing the temperature from 313 K to 523 K at 400 bar increased the mole fraction solubility of benzo[ghi]perylene from 3.3×10^{-7} to 4.55×10^{-4} compared to an increase from 2.9×10^{-6} to 4.55×10^{-4} when the pressure was increased from 100 bar to 450 bar at 523 K. Correlation of the results shows good self-consistency of the data obtained and reasonable agreement with the available published data. Equations are given for the solubilities over the pressure and temperature conditions studied.

Introduction

Supercritical carbon dioxide (CO₂) has gained increasing attention for applications such as extracting polycyclic aromatic hydrocarbons (PAHs) and other contaminants from soils and sludges for either analytical or remediation purposes. A factor limiting the application of this technology is the lack of fundamental solubility data needed to design separation units or to develop extraction models. Data are especially limited on the effect of elevated temperature on the solubility of organic compounds in CO₂, even though analytical scale extractions of soils and sludges have shown that increasing the extraction temperature is usually much more effective than increasing pressure for extracting polycyclic aromatic hydrocarbons (PAHs), polychlorinated biphenyls (PCBs), and a variety of different classes of organic pollutants (Hawthorne and Miller, 1994; Yang et al., 1995; Langenfeld et al., 1995). In a recent review by Bartle et al. (1991), and in recent literature, more than 2500 data points for the solubility of organic compounds in supercritical CO₂ over a temperature range of 305 K to 373 K have been reported; however, very few solubilities have been reported at temperatures over 373 K (Kosal et al., 1992; Sheng et al., 1992; Foster et al., 1993; Madras et al., 1993; Reverchon et al., 1993; Ashour and Hammam, 1993; Staby and Mollerup, 1993; Bamberger and Maurer, 1994; Quiram et al., 1994; Borch-Jensen et al., 1994; Cowey et al., 1995; Suoqi et al., 1995). This paper reports the solubility of four PAHs (pyrene, chrysene, perylene, and benzo[ghi]perylene) at temperatures between 313 K and 523 K and pressures from 100 bar to 450 bar. The solubility determinations were performed with an on-line flame ionization detector method developed in our laboratory (Miller and Hawthorne, 1995) which allows PAH mole fraction solubilities to be determined from $x \approx 10^{-7}$ to 10^{-2} . The results are correlated using the concept of solubility enhancement (Johnston et al., 1989)

Experimental Section

All solubility measurements were performed using an on-line flame ionization detector (FID) method developed

in our laboratory. A detailed description of the construction, calibration, and validation of this method has been previously reported (Miller and Hawthorne, 1995). Briefly, a high-pressure saturation cell (either 0.167, 0.498, or 1.67 mL, Keystone Scientific, Bellefonte, PA) was filled with a 5 mass % mixture of the compound with clean sea sand. The saturation cell was placed in the oven of a Hewlett-Packard Model 5890 gas chromatograph (Hewlett-Packard, Wilmington, DE) to provide precise temperature control (± 0.1 °C according to manufacturer's specifications) during the solubility determination. An ISCO Model 100D syringe pump (ISCO, Lincoln, NE) fitted with a constant temperature jacket maintained at 27 °C was used in the constant pressure mode to supply pressurized CO₂ via a 3-m preheating coil (placed in the GC oven) to the saturation cell. An ISCO stainless steel restrictor (300 μm o.d. \times 57 μm i.d., 40 cm long) was attached to the outlet of the saturation cell to control the CO₂ flow. Since the relatively large inside diameter (57 μm) of the restrictor allows too much CO₂ flow for the FID to accommodate, the end of the restrictor was crimped to adjust the flow to approximately 150 $\mu\text{L}/\text{min}$ liquid CO₂ at 400 bar and 25 °C (flow measured as liquid CO₂ at the pump). The restrictor outlet was inserted into a volatilization chamber maintained at 400 °C where the CO₂ and the compound are vaporized before entering the FID supplied with the GC. Details of the construction of the volatilization chamber are given in Miller and Hawthorne (1995). CO₂ flow data were acquired with a personal computer using the RS-232 interfacing capabilities of the ISCO 100D pump.

Five mass percent mixtures of either pyrene, chrysene, perylene, or benzo[ghi]perylene (Aldrich Chemical, Milwaukee, WI) with washed sea sand were used to fill the saturation cell for each determination. All compounds were of the highest purity available (>98%, confirmed by gas chromatographic analysis). Solubility determinations were performed at temperatures of 313 K to 523 K and pressures from 100 bar to 450 bar. During a typical experiment, the oven temperature was held constant while the pressure was raised in 50 bar increments. Each pressure was held

Table 1. Density of Supercritical CO₂ for Temperatures and Pressures Used for PAH Solubility Determinations

P/bar	$\rho/\text{kg m}^{-3}$ ^a				
	313 K	373 K	423 K	473 K	523 K
100	607	188	144	121	106
150	789	331	231	188	161
200	847	470	324	256	217
250	886	583	415	324	271
300	919	662	491	387	323
350	942	715	554	444	371
400	962	755	606	493	414
450	981	789	651	537	454

^a Calculated densities were obtained using a modified equation of state which was extended to include high-pressure fluids based on the method of Pitzer (1955) and Pitzer et al. (1955) and used in the ISCO "SF-Solver", as confirmed experimentally by Langenfeld et al. (1992).

Table 2. Mole Fraction Solubility (10⁶x) of Benzo[ghi]perylene in Supercritical CO₂^a

/bar	T/K				
	313	373	423	473	523
100	<i>b</i>	<i>b</i>	<i>b</i>	1.7	2.9 ± 0.2
150	<i>b</i>	0.15	0.26	2.5	9.7 ± 1.4
200	<i>b</i>	0.43	1.9	6.8	29.3 ± 2.1
250	0.18 ± 0.03	1.6	5.2	16	63.3 ± 1.1
300	0.27 ± 0.02	2.7	11	37	123 ± 3
350	0.31 ± 0.02	4.0	18	57	231 ± 10
400	0.33 ± 0.02	4.8	30	87	326 ± 12
450	ND ^c	5.4	38	108	455

Standard deviations (SD) are based on triplicate determinations at each condition. Values without SDs listed are single determinations. ^b Solubility was less than the reliable detection limit of $x = 1 \times 10^{-7}$. ^c Not determined.

Table 3. Mole Fraction Solubility (10⁶x) of Perylene in Supercritical CO₂^a

/bar	T/K				
	313	373	423	473	523
100	<i>b</i>	<i>b</i>	<i>b</i>	1.1	31.0 ± 0.8
150	<i>b</i>	<i>b</i>	<i>b</i>	4.0	34.4 ± 0.3
200	<i>b</i>	<i>b</i>	0.73	11	66 ± 1
250	<i>b</i>	1.2	4.6	27	118 ± 4
300	0.33 ± 0.01	3.6	12	43	197 ± 5
350	0.72 ± 0.02	6.1	24	95	330 ± 14
400	0.93 ± 0.02	9.0	38	154	479 ± 18
450	1.40 ± 0.07	12.0	56	217	700 ± 13

Standard deviations (SD) are based on triplicate determinations at each condition. Values without SDs listed are single determinations. ^b Solubility was less than the reliable detection limit of $x = 3 \times 10^{-7}$.

for at least 10 min after both the CO₂ flow readings and the FID signal stabilized (see Miller and Hawthorne (1995) for details of the procedure). The FID signal typically stabilized (i.e., variations in signal were <5%) in <1 min after changing pressures. Because of the CO₂ compressibility, the flow readings typically required 5–10 min to stabilize after a pressure change at 100 bar and 150 bar, and approximately 3 min at all higher pressures.

Prior to any solubility determination, the response of the FID for anthracene was determined to ensure day-to-day stability of the detector. This was accomplished by weighing approximately 2 mg of anthracene into a 0.167-mL cell, passing CO₂ at a high-solubility condition (472 K and 400 bar; Miller and Hawthorne, 1995) through the cell, and recording the FID signal until it returned to baseline (i.e., all of the anthracene was eluted). FID response (mass chart paper/mass anthracene) varied <±5% over the course of this investigation (~1 year). Any large deviation in FID

Table 4. Mole Fraction Solubility (10⁵x) of Chrysene in Supercritical CO₂^a

P/bar	T/K				
	313	373	423	473	523
100	<i>b</i>	<i>b</i>	<i>b</i>	0.6	7.5 ± 0.8
150	<i>b</i>	<i>b</i>	<i>b</i>	2.5	23 ± 4
200	<i>b</i>	0.6	0.7	5.4	38 ± 4
250	0.22 ± 0.01	1.2	1.7	11	77 ± 11
300	0.27 ± 0.004	2.1	3.5	22	146 ± 14
350	0.33 ± 0.01	2.7	6.3	41	229 ± 6
400	0.41 ± 0.02	3.0	10	65	310 ± 6
450	0.46 ± 0.02	3.3	15	116	361 ± 9

^a Standard deviations (SD) are based on triplicate determinations at each condition. Values without SDs listed are single determinations. ^b Solubility was less than the reliable detection limit of $x = 2 \times 10^{-6}$.

Table 5. Mole Fraction Solubility (10⁵x) of Pyrene in Supercritical CO₂^a

P/bar	T/K			
	313	373	423 ^b	473 ^b
100	0.61 ± 0.16	1.6	5.9 ± 0.3	ND ^c
150	4.6 ± 1.0	2.2	9.7 ± 0.9	22 ± 7
200	9.9 ± 0.6	13	27 ± 3	49 ± 7
250	14.2 ± 1.5	38	63 ± 3	101 ± 15
300	18 ± 2	68	135 ± 9	185 ± 11
350	23 ± 1	101	238 ± 17	278 ± 10
400	27 ± 1	123	332 ± 4	394 ± 31
450	30 ± 1	156	424 ± 2	479 ± 24

^a Standard deviations (SD) are based on triplicate determinations at each condition. Values without SDs listed are single determinations. ^b Since the normal melting point of pyrene is 423 K, the data at 473 K (and likely 423 K) no longer represent a solid supercritical CO₂ system but rather represent the equilibrium vapor phase over liquid pyrene which is saturated with CO₂. ^c Not determined.

response for anthracene indicated a problem with the system (i.e., plugged restrictor or contaminated FID) and was corrected before proceeding. In addition to the daily anthracene calibrations, daily calibrations for each compound were performed in an identical manner with day-to-day variations of <±5%.

Results and Discussion

Effect of Pressure and Temperature on PAH Solubilities. The densities of CO₂ calculated by the ISCO "SF-Solver" at the various pressure and temperature conditions used for the PAH solubility determinations are shown in Table 1. (The ISCO "SF-Solver" uses the modified equation of state extended to include high-pressure fluids as proposed by Pitzer (1955) and Pitzer et al. (1955)). The solubilities of benzo[ghi]perylene (molecular weight = 276, normal melting point = 551 K), perylene (molecular weight = 252, normal melting point = 534 K), chrysene (molecular weight = 228, normal melting point = 525 K), and pyrene (molecular weight = 202, normal melting point = 423 K) at pressures ranging from 100 bar to 450 bar and temperatures from 313 K to 523 K are shown in Tables 2–5. With the exception of pyrene (Table 5), all solubility determinations were performed at temperatures below the normal melting point of the pure compound.

The data in Tables 2–5 and in Figure 1 show that, in general, increasing temperature has a much more dramatic effect on the solubility of PAHs than does increasing pressure. For example, the mole fraction solubility of benzo[ghi]perylene (Table 2 and Figure 1) at 400 bar

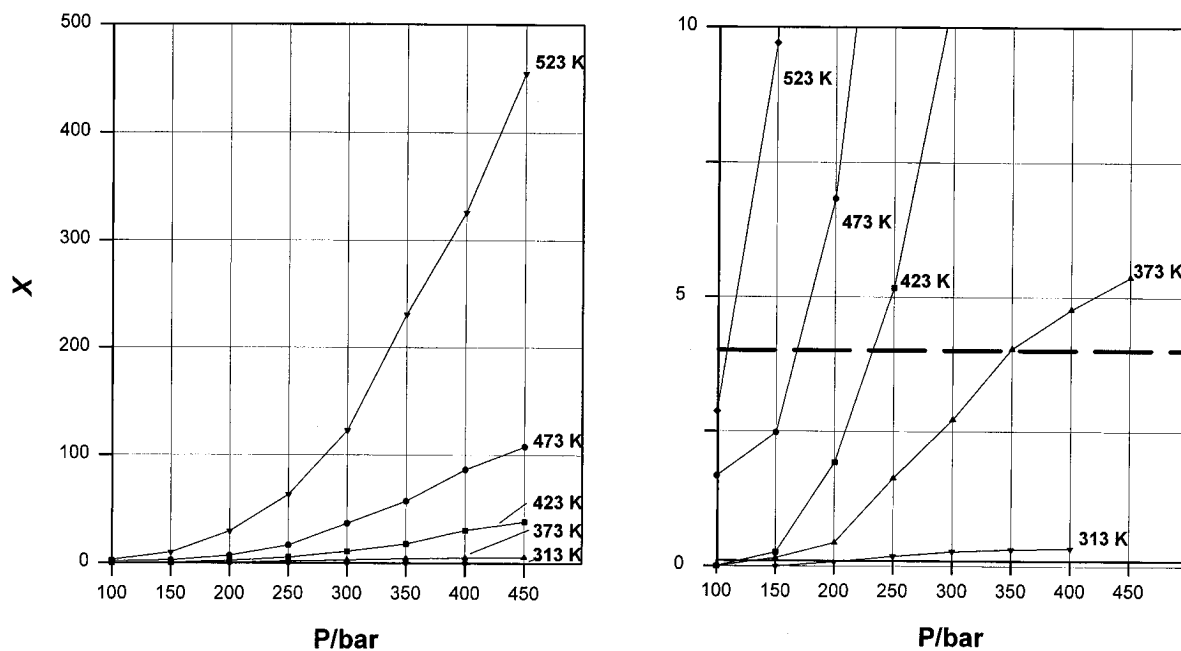


Figure 1. Effect of temperature and pressure on the solubility of benzo[ghi]perylene from 100 bar to 450 bar and 313 K to 523 K. The right side of the figure is expanded to show the lower-solubility results. The dashed line indicates constant mole fraction solubility conditions $\times 10^{-6}$. The full data set (left) is expanded for the lower-solubility conditions (right).

increases from 3.3×10^{-7} at 313 K to 3.26×10^{-4} at 523 K, an increase of nearly 3 orders of magnitude, even though the density of the supercritical CO_2 decreases from 962 kg m^{-3} to 414 kg m^{-3} . In contrast, increasing pressure at 373 K (a typical upper temperature for solubility data in the literature) raises the mole fraction solubility of benzo[ghi]perylene from 1.5×10^{-7} at 150 bar to 5.37×10^{-6} at 450 bar, an increase of only 36-fold. Similar increases in solubility with increasing temperature occur for perylene and chrysene (Tables 3 and 4). Increasing the temperature from 313 K to 523 K (at constant pressure) increases the mole fraction solubility of perylene by a factor of at least 100 (at lower pressures) to ~ 500 (at higher pressures). Similarly, increasing the temperature from 313 K to 523 K (at constant pressure) increases the mole fraction solubility of chrysene by a factor of 350 (at 250 bar) to ~ 800 (at higher pressures).

To determine the effect on the solubility of a PAH which is above its melting point at the higher temperatures used in this study, the final solubility determinations were performed with pyrene (molecular weight = 202, normal melting point = 423 K). As shown in Table 5, the solubility of pyrene increases with temperatures up to 423 K in a manner similar to the solubility increases shown for benzo[ghi]perylene, perylene, and chrysene shown in Tables 2–4. However, when the temperature is increased from 423 K to 473 K, the solubility of pyrene increases only slightly at all pressures studied. Such results might be expected since the results at 473 K no longer represent a solid/supercritical CO_2 system but rather represent the equilibrium vapor phase over liquid pyrene which is saturated with CO_2 (McHugh and Krokonis, 1986, Chapter 3). It is also possible that the data at 423 K represent the liquid pyrene case since the normal melting point of pyrene is 423 K.

In the majority of SFE studies to date, attempts to increase PAH solubilities have focused on increasing pressure at lower temperatures in order to maximize the CO_2 density. This approach is often based on the popular correlation parameter originally proposed by Giddings et al. (1968), relating increased CO_2 density to a higher solubility. While increasing pressure (at constant temper-

ature) certainly does increase PAH solubilities, the results in Tables 2–5 clearly demonstrate that increasing temperature (at constant pressure) causes much higher increases in PAH solubilities despite the drop in CO_2 density which occurs at constant pressure (Table 1). Although such solubility increases for heavy solids with temperature might be expected on the basis of known phase behavior (McHugh and Krokonis, 1986, Chapter 3), the results in Tables 2–5 are the first to experimentally determine solubilities over a wide temperature range.

Estimation of Constant Solubility Conditions. The data in Tables 2–5 enables one to estimate temperature/pressure combinations that produce constant solubility conditions (e.g., which could be useful for engineering design purposes where raising temperature may be less expensive than raising pressure). For example, benzo[ghi]perylene has a mole fraction solubility of 4×10^{-6} at all of the temperature/pressure conditions indicated by the dashed line in Figure 1. For example, the pressure required to achieve a mole fraction solubility of 4×10^{-6} for perylene solubility at 313 K is 433 bar. However, the same mole fraction solubility can be obtained at only 104 bar if the temperature is raised to 473 K.

Correlation of the Results. The correlations were based on the concept of solubility enhancement (Johnston et al., 1989) from which the following equations were derived (Bartle et al., 1991):

$$\ln(xp/p_{\text{ref}}) = A + c(\rho - \rho_{\text{ref}}) \quad (1)$$

where x is the mole fraction of the solute (taken here to be equal to the ratio of the number of moles of solute divided by the number of moles of carbon dioxide), p is the pressure, p_{ref} is 1 bar, ρ is the density (taken as the density of pure carbon dioxide), ρ_{ref} is 700 kg m^{-3} , and A and c are constants. ρ_{ref} is used so that the intercept A is within the experimental data range and does not suffer the variability experienced if an intercept extrapolated to zero density is used (Bartle et al., 1991). The constant c , resulting physically from solvation by the fluid, is assumed to be constant over the temperature range and the constant A ,

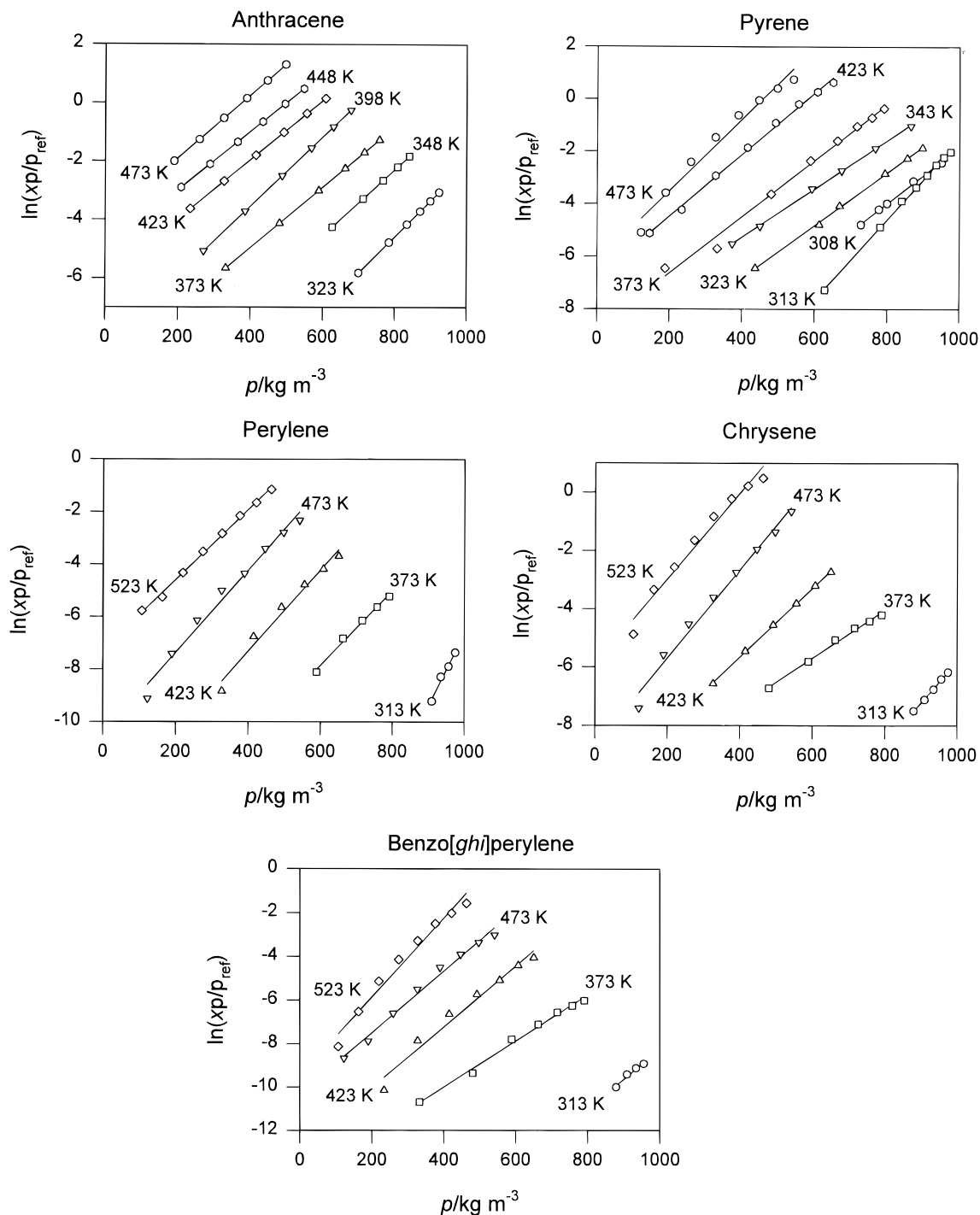


Figure 2. Plots of isotherms of $\ln(xp/p_{ref})$ versus density for five PAHs.

arising from the vapor pressure (fugacity) of the solute, is assumed to obey the equation

$$A = a + b/T \quad (2)$$

where a and b are constants and T is the absolute temperature. When eqs 1 and 2 are combined, the overall correlation equation is obtained to be

$$\ln(xp/p_{ref}) = a + b/T + c(\rho - \rho_{ref}) \quad (3)$$

The results presented in this paper, previously published data on anthracene (Miller et al., 1995) obtained by the same experimental method, and for comparison, published

data for pyrene (Johnston et al., 1982) have been fitted to the above equations. The initial stage is to plot $\ln(xp/p_{ref})$ for each isotherm against density (Figure 2) and fit the plots to a straight line by least squares to obtain A (the value of the fitted line at ρ_{ref}) and c . These plots are expected to be reasonably straight lines of similar slopes. This is seen to be the case for anthracene, and the situation would be improved further if the lowest density points at 373 K and 398 K were ignored. For pyrene, the four isotherms obtained in the present study are shown with data obtained at 308 K, 323 K, and 343 K obtained by Johnston et al. (1982). Reasonably straight lines are obtained for all isotherms except at the highest temperature, which is above the melting point of pyrene (423 K) and where the correlation method is expected to be less

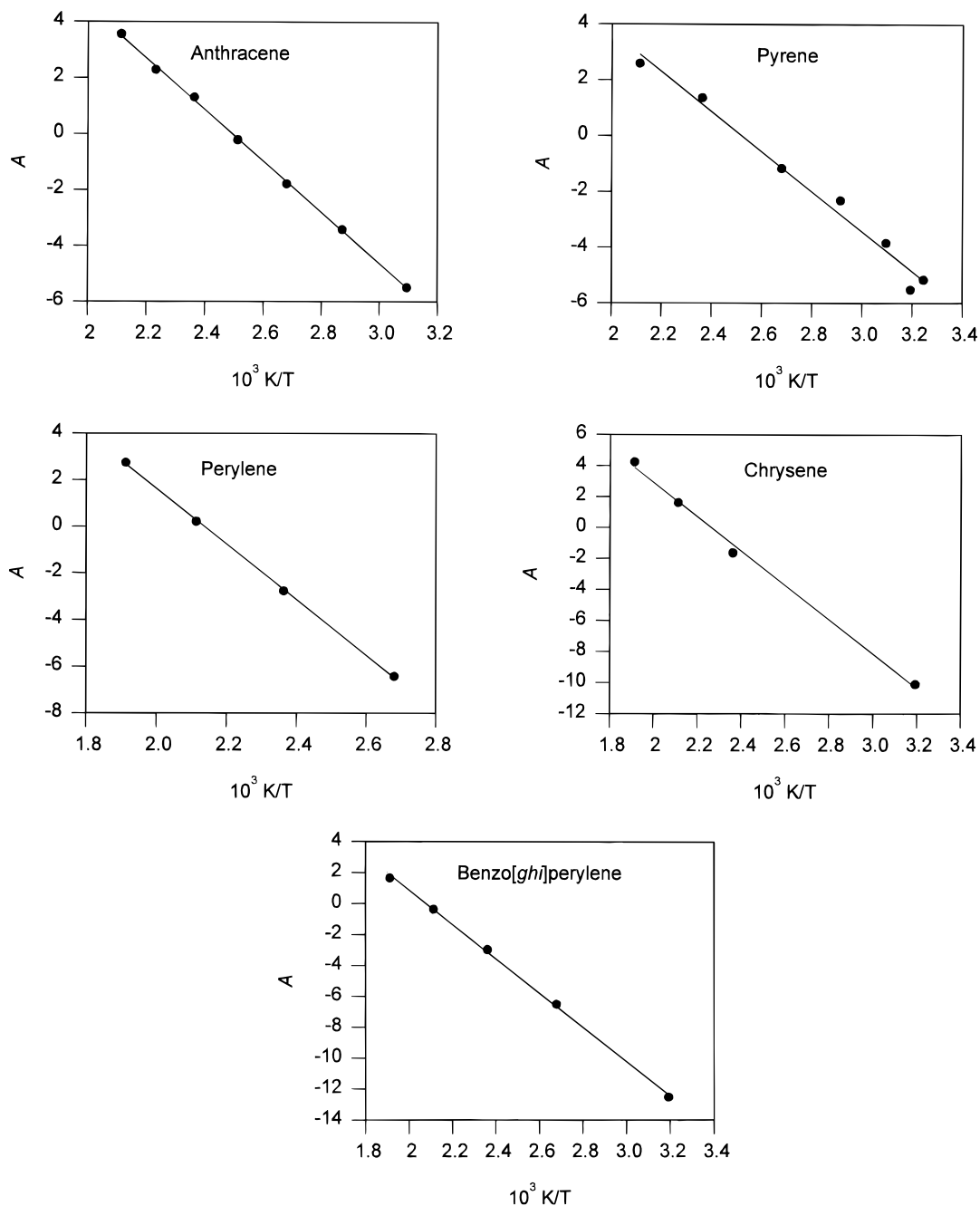


Figure 3. Plots of the isotherm intercept, A , versus $1/T$ for five PAHs.

successful. However, the slopes of the lines are less constant and there is a tendency for the slopes for the present data to be greater than those for the data of Johnston et al. (1982). Nevertheless, there is a measure of consistency between the two sets of data. For perylene, there is a reasonable fit with constant slope, which again would be improved if some of the low solubilities were excluded. For chrysene, the situation is also acceptable except for the isotherm at 373 K, where the slope is markedly different. There was no experimental explanation for the inconsistency, which remains unexplained. Benzo[ghi]perylene showed rather more curved plots, which again could be improved by being selective about some of the lower-pressure measurements. Although, in general, plots could be improved by removing lower-pressure points, the decision was taken not to do this unless there were experimental reasons.

Table 6. Constants in Eq 3 Obtained from Data Correlation^a

	a	b/K	$c/m^3 \text{ kg}^{-1}$
anthracene (489 K)	22.66	-9 078	0.010 96
pyrene (423 K)	19.02	-7 512	0.011 60
perylene (534 K)	25.50	-11 938	0.014 96
chrysene (526 K)	25.21	-11 187	0.014 35
benzo[ghi]perylene (551 K)	22.97	-11 058	0.014 33

^a Melting points are shown in brackets after each compound.

Choices were then made about which isotherms to include in further analysis. For anthracene, all data were included. For pyrene, various combinations were tried of which none was very successful. It was, therefore, decided to include all data, including those of Johnston et al. (1982). For perylene, the data at 313 K were obtained from only four solubilities which were low and looked inconsistent in Figure 2, and so this isotherm was excluded. For chrysene, the isotherm at 373 K, which had previously been

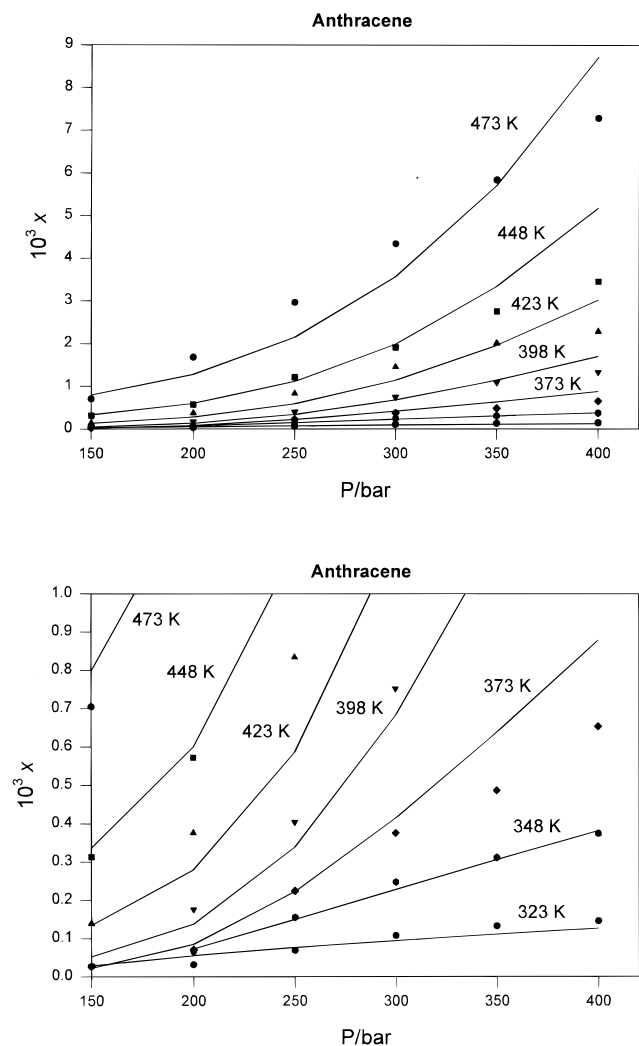


Figure 4. Comparison of experimental solubilities for anthracene versus pressure, shown as points (Miller, et al., 1995), with the predictions of eq 3 using the parameters of Table 6, shown as lines. The full data set (top) is expanded for the lower-solubility conditions (bottom).

described as having an inconsistent slope, was excluded. For benzo[ghi]perylene, all isotherms were used.

The values of c , obtained from the included isotherms, were then averaged for each compound. The experimental data for the chosen isotherms were used, now holding c at the average value, to obtain the best values of A . Plots of

versus $1/T$ were then fitted to straight lines to obtain the constants a and b for the five compounds and are shown in Figure 3. A good straight line was obtained for all compounds except for a rather scattered plot for pyrene, because of the inclusion of both sets of data. The averaged values of c as well as values of a and b obtained from the plots versus $1/T$ are given in Table 6.

These values were then used to predict solubilities from eq 3, and the values obtained are plotted as lines and compared with the experimental data, shown as points, in Figures 4–8. Two plots for each compound are given to show comparisons for both high and low solubility values. Comparisons are made for all data, including those that were excluded when obtaining the parameters in Table 6. Agreement is seen to be sometimes good, and poor agreement is mainly limited to (a) data for isotherms which have previously been excluded, (b) data for isotherms above or close to melting points for anthracene (489 K) and pyrene (423 K), and (c) pyrene where there is some disagreement between the two sets of data.

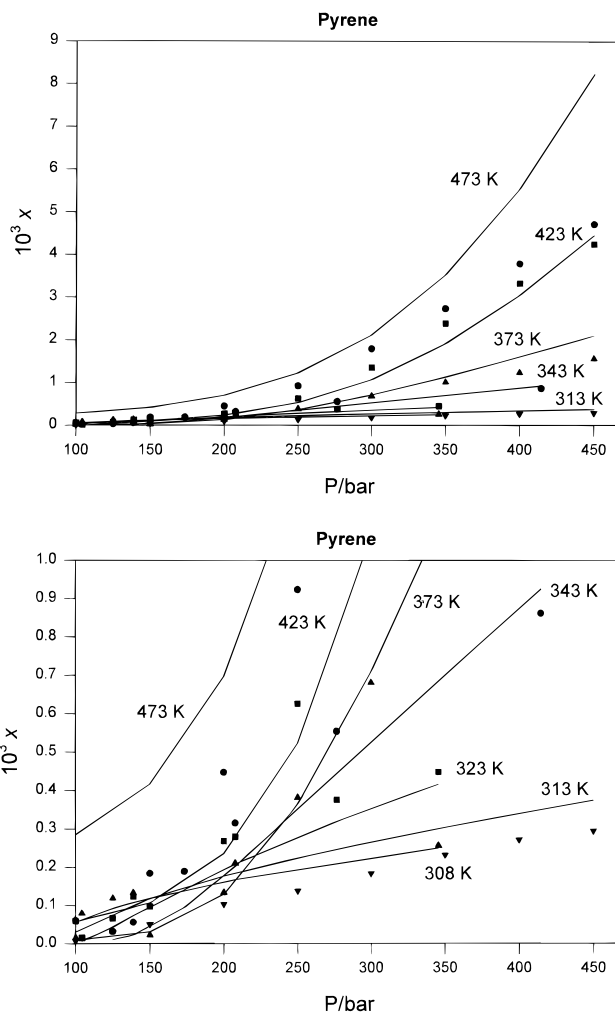


Figure 5. Comparison of experimental solubilities for pyrene versus pressure, shown as points, with the predictions of eq 3 using the parameters of Table 6, shown as lines. Isotherms at 308 K, 323 K, and 343 K are the data of Johnston et al. (1982), and the other isotherms are from the present study. The full data set (top) is expanded for the lower-solubility conditions (bottom). Since the normal melting point of pyrene is 423 K, the data at 473 K (and likely 423 K) no longer represent a solid supercritical CO_2 system but rather represent the equilibrium vapor phase over liquid pyrene which is saturated with CO_2 .

Where a solute is liquid, the equilibrium involved is that between a solute-rich liquid phase and a fluid phase rich in carbon dioxide, rather than a straightforward solubility. Even below the melting point of the solute, solute-rich liquid phases may be formed in the presence of carbon dioxide under pressure. For example, it is known that, although the melting point of naphthalene is 354 K, a liquid phase is formed in the presence of pressurized carbon dioxide and at temperatures above 338 K (McHugh and Paulaitis, 1980). Corresponding data are not available for the compounds discussed here, but it can be assumed that the correlation may not be as valid above temperatures 30 K less than the melting points of the compounds, shown in brackets in Table 6. At other temperatures, discrepancies will be due partly to the failure of the correlation and partly to experimental error in the data used. There will be some averaging of experimental errors by the correlation, and it is suggested that, below 30 K less than the melting point, predictions of solubility made using eq 3 and the parameters of Table 6 have a probable error of 10% to 20%.

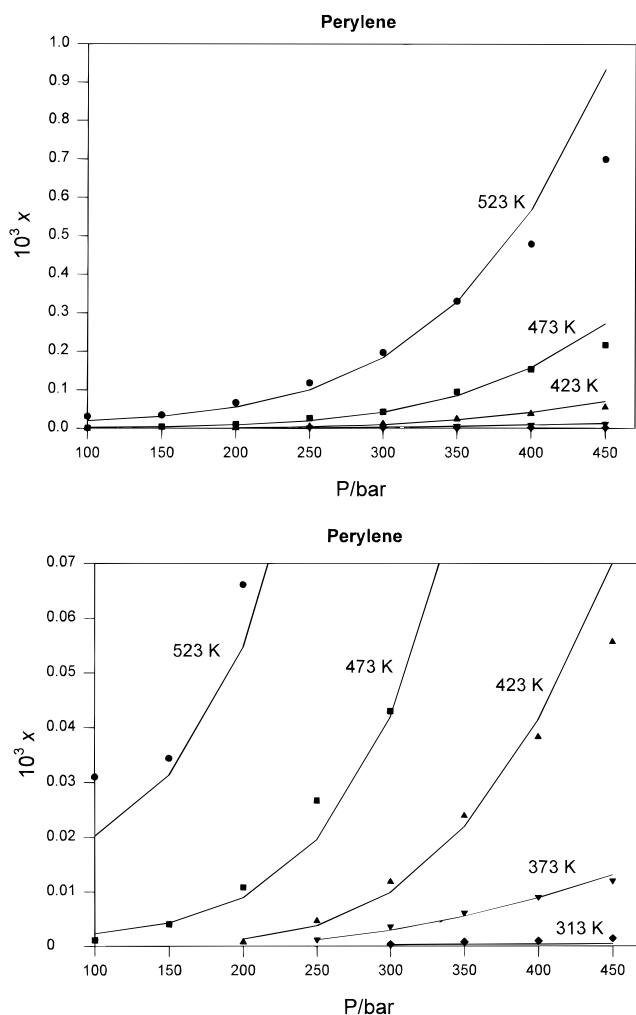


Figure 6. Comparison of the reported experimental solubilities for perylene versus pressure, shown as points, with the predictions of eq 3 using the parameters of Table 6, shown as lines. The full data set (top) is expanded for the lower-solubility conditions (bottom).

Table 7. Comparison of values of $\Delta_{\text{vap}}H/\text{kJ mol}^{-1}$ Obtained from Eq 4 with Published Values

	eq 4	published ^a
anthracene	76	74
pyrene	63	65
perylene	99	129
chrysene	93	117
benzo[ghi]perylene	92	

Data taken from Jones, 1960.

The parameter b is approximately related to the enthalpy of vaporization of the solid, $\Delta_{\text{vap}}H$, by

$$\Delta_{\text{vap}}H = -Rb \quad (4)$$

where R is the gas constant. The validity of eq 4 relies on the assumption that the enhancement factor $\ln(xp/p_v)$, where p_v is the vapor pressure of the solid solute, is independent of temperature, which is found to be only approximately true in practice. For naphthalene, where there are many solubility data, eq 4 gives a value of $\Delta_{\text{vap}}H$ of 77 kJ mol^{-1} compared with a published value of 70 kJ mol^{-1} (Bartle et al., 1991). Comparison for the compounds studied here of $\Delta_{\text{vap}}H$ obtained using eq 4 with published values, where available, is shown in Table 7 and gives a

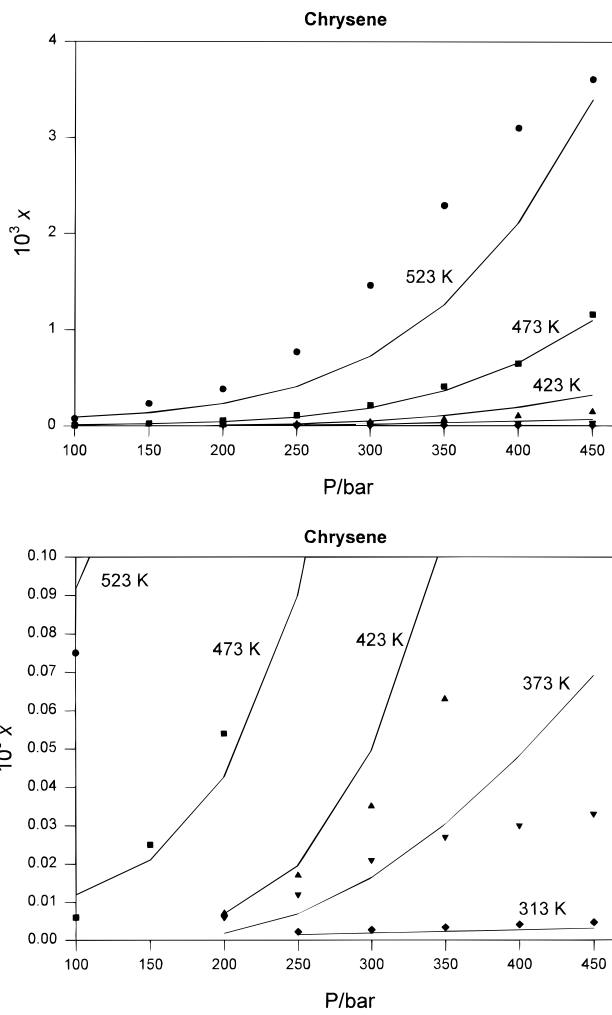


Figure 7. Comparison of the reported experimental solubilities for chrysene versus pressure, shown as points, with the predictions of eq 3 using the parameters of Table 6, shown as lines. The full data set (top) is expanded for the lower-solubility conditions (bottom).

similar degree of agreement. This gives further confidence in the solubility results obtained.

Conclusions

The solubilities of PAHs in supercritical CO_2 increase much more rapidly with higher temperatures (at constant P) than with higher pressures (at constant T) over pressures from 100 bar to 450 bar and temperatures from 313 K to 523 K. For low-solubility PAHs such as perylene and benzo[ghi]perylene, solubility enhancements of 500–1000-fold can be accomplished by raising the temperature from 313 K to 523 K at 400 bar, while raising the pressure from 100 bar to 450 bar has much less effect in increasing solubilities, particularly at lower temperatures. Correlation using eq 3 shows that the majority of the experimental data is self-consistent, given the straight line plots for the isotherms, their approximately constant slopes, and the behavior of their intercepts with respect to temperature. Agreement with previous literature data for pyrene was fair. Parameters were obtained which allow predictions of solubility with a probable error of 10–20% over much of the temperature range. It should be noted that the predictions have been made over a wide temperature and pressure range using only three parameters for each compound, while much more sophisticated correlations based on equations of state are only successful over smaller ranges of conditions (Johnston, et al. 1989).

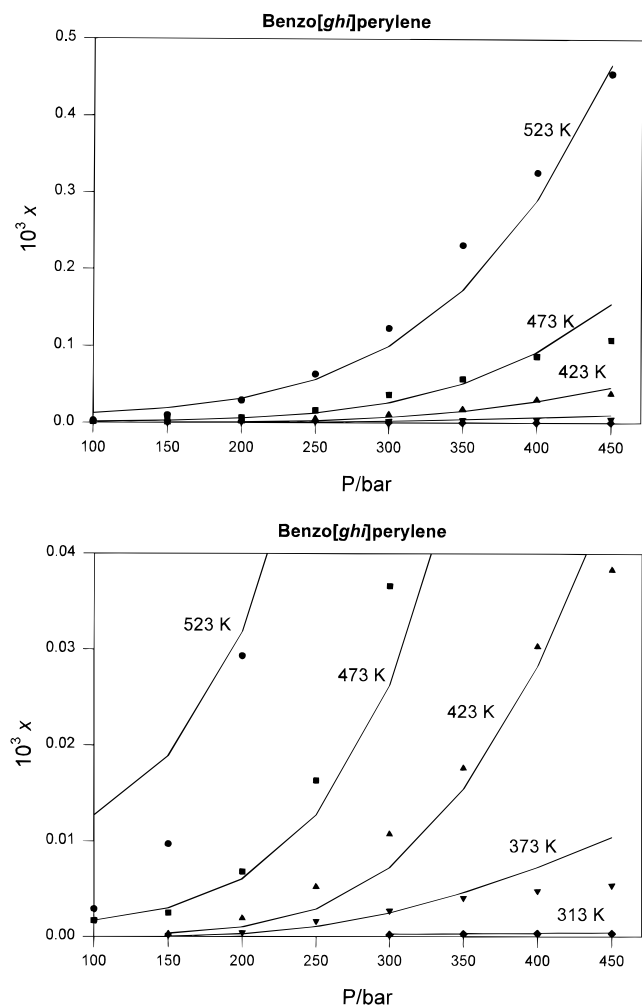


Figure 8. Comparison of the reported experimental solubilities for benzo[ghi]perylene versus pressure, shown as points, with the predictions of eq 3 using the parameters of Table 6, shown as lines. The full data set (top) is expanded for the lower-solubility conditions (bottom).

Acknowledgment

The authors would like to thank ISCO for instrument loans and for the restrictors used in this study.

Literature Cited

- Ashour, I.; Hammam, H. Equilibrium Solubility of Pure Mono-, Di-, and Trilaurin in Supercritical Carbon Dioxide – Experimental Measurements and Model Prediction. *J. Supercrit. Fluids* **1993**, *6*, 8.
- Bamberger, A.; Maurer, G. High-Pressure Vapor-Liquid Equilibria in Binary Mixtures of Carbon Dioxide and Aromatic Hydrocarbons: Experimental Data and Correlation for CO₂ + Acetophenone, CO₂ + 1-chloronaphthalene, CO₂ + Methyl Benzoate and CO₂ + *n*-Propylbenzene. *J. Supercrit. Fluids* **1994**, *7*, 115–127.
- Bartle, K. D.; Clifford, A. A.; Jafar, S. A.; Shilstone, G. F. Solubilities of Solids and Liquids of Low Volatility in Supercritical Carbon Dioxide. *J. Phys. Chem. Ref. Data* **1991**, *20* (4), 713–756.
- Borch-Jensen, C.; Staby, A.; Møllerup, J. Mutual Solubility of 1-Butanol and Carbon Dioxide, Ethene, Ethane, or Propane at a Reduced Supercritical Solvent Temperature of 1.03. *J. Supercrit. Fluids* **1994**, *7*, 231–244.

- Cowey, C. M.; Bartle, K. D.; Burford, M. D.; Clifford, A. A.; Zhu, S.; Smart, N. G.; Tinker, N. D. Solubility of Ferrocene and a Nickel Complex in Supercritical Fluids. *J. Chem. Eng. Data* **1995**, *40*, 1217–1221.
- Foster, N. R.; Singh, H.; Yun, S. L. J.; Tomasko, D. L.; Macnaughton, S. J. Polar and Nonpolar Cosolvent Effects on the Solubility of Cholesterol in Supercritical Fluids. *Ind. Eng. Chem. Res.* **1993**, *32*, 2849–2853.
- Giddings, J. C.; Meyer, M. N.; McLaren, L.; Keller, R. A. High Pressure Gas Chromatography of Nonvolatile Species. *Science* **1968**, *162*, 67–73.
- Hawthorne, S. B.; Miller, D. J. Direct Comparison of Soxhlet and Low- and High-Temperature CO₂ Extraction Efficiencies of Organics from Environmental Solids. *Anal. Chem.* **1994**, *66*, 4005–4012.
- Johnston, K. P.; Ziger, D. H.; Eckert, C. A. Solubilities of Hydrocarbon Solids in Supercritical Fluids. The Augmented van der Waals Treatment. *Ind. Eng. Chem. Fundam.* **1982**, *21*, 191–197.
- Johnston, K. P.; Peck, D. G.; Kim, S. Modeling Supercritical Mixtures: How Predictive Is It? *Ind. Eng. Chem. Res.* **1989**, *28*, 1115–1125.
- Jones, A. H. Sublimation Pressure Data for Organic Compounds. *J. Chem. Eng. Data* **1960**, *5*, 196–200.
- Kosal, E.; Lee, C. H.; Holder, G. D. Solubility of Progesterone, Testosterone, and Cholesterol in Supercritical Fluids. *J. Supercrit. Fluids* **1992**, *5*, 169–179.
- Langenfeld, J. J.; Hawthorne, S. B.; Miller, D. J.; Tehrani, J. Method for Determining the Density of Pure and Modified Supercritical Fluids. *Anal. Chem.* **1992**, *64*, 2263–2266.
- Langenfeld, J. J.; Hawthorne, S. B.; Miller, D. J. Kinetic Study of Supercritical Fluid Extraction of Organic Contaminants from Heterogeneous Environmental Samples with Carbon Dioxide and Elevated Temperatures. *Anal. Chem.* **1995**, *34*, 1727–1736.
- Madras, G.; Erkey, C.; Akgerman, A. A New Technique for Measuring Solubilities of Organics in Supercritical Fluids. *J. Chem. Eng. Data* **1993**, *38*, 422–423.
- McHugh, M. A.; Paulaitis, M. E. Solid Solubilities of Naphthalene and Biphenyl in Supercritical Carbon Dioxide. *J. Chem. Eng. Data* **1980**, *25*, 326–329.
- McHugh, M. A.; Krukoni, V. J. *Supercritical Fluid Extraction: Principles and Practice*; Butterworths: Stoneham, MA, 1986.
- Miller, D. J.; Hawthorne, S. B. Determination of Solubilities of Organic Solutes in Supercritical CO₂ by On-Line Flame Ionization Detection. *Anal. Chem.* **1995**, *67*, 273–279.
- Pitzer, K. S. The Volumetric and Thermodynamic Properties of Fluids. I. Theoretical Basis and Virial Coefficients. *J. Am. Chem. Soc.* **1955**, *77*, 3427–3433.
- Pitzer, K. S.; Lippman, D. Z.; Curl, R. F., Jr.; Huggins, C. M.; Petersen, D. E. The Volumetric and Thermodynamic Properties of Fluids. II. Compressibility Factor, Vapor Pressure and Entropy of Vaporization. *J. Am. Chem. Soc.* **1955**, *77*, 3433–3440.
- Quiram, D. J.; O'Connell, J. P.; Cochran, H. D. The Solubility of Solids in Compressed Gases. *J. Supercrit. Fluids* **1994**, *7*, 159–164.
- Reverchon, E.; Russo, P.; Stassi, A. Solubilities of Solid Octacosane and Triacontane in Supercritical Carbon Dioxide. *J. Chem. Eng. Data* **1993**, *38*, 458–460.
- Sheng, Y. J.; Chen, P. C.; Chen, Y. P.; Wong, D. S. H. Calculations of Solubilities of Aromatic Compounds in Supercritical Carbon Dioxide. *Ind. Eng. Chem. Res.* **1992**, *31*, 967–973.
- Staby, A.; Møllerup, J. Measurement of Mutual Solubilities of 1-Pentanol and Supercritical Carbon Dioxide. *J. Supercrit. Fluids* **1993**, *6*, 15–19.
- Suoqi, Z.; Renan, W.; Guanghua, Y. A Method for Measurement of Solid Solubility in Supercritical Carbon Dioxide. *J. Supercrit. Fluids* **1995**, *8*, 15–19.
- Yang, Y.; Gharaibeh, A.; Hawthorne, S. B.; Miller, D. J. Combined Temperature/Modifier Effects on Supercritical CO₂ Extraction Efficiencies of Polycyclic Aromatic Hydrocarbons from Environmental Samples. *Anal. Chem.* **1995**, *67*, 641–646.

Received for review January 25, 1996. Accepted April 1, 1996. Partial funding for this work was provided by the U.S. Environmental Protection Agency (RREL, Cincinnati, OH). The authors thank the EPSRC (U.K.) for financial support of the correlation work.

JE960022U

Abstract published in *Advance ACS Abstracts*, May 15, 1996.